J Appl Electrochem (2011) 41:115–121
DOI 10.1007/s10800-010-0219-2

ORIGINAL PAPER

Application of cobalt oxide nanoparticles as an electron transfer facilitator in direct electron transfer and biocatalytic reactivity of cytochrome *c*

Ali Mohammadi · Abdolmajid Bayandori Moghaddam · Sara Ahadi · Rassoul Dinarvand · Abbas Ali Khodadadi

Received: 7 December 2009 / Accepted: 5 September 2010 / Published online: 8 October 2010

Abstract We describe a modification of glassy carbon (GC) electrode surface with electrodeposited cobalt oxide nanoparticles (CoOx NPs), and then, this electrode is used to immobilization of Cytochrome *c* (Cyt *c*). The morphology of electrodeposited CoOx NPs was analyzed by scanning electron microscopy (SEM) and atomic force microscopy (AFM). Electrochemical redox property investigation of immobilized protein (Cyt *c*) molecules was accomplished by cyclic voltammetry (CV) technique. Cyt *c*/CoOx NPs/GC electrode exhibits electron transfer between the protein prosthetic groups and electrodeposited nanoparticles on the electrode surface and displayed a couple of stable redox peaks with a formal potential ($E^{o'}$) of −89.5 mV (107.5 mV vs. NHE) with respect to reference electrode in 0.05 M phosphate buffer solution (pH 7.0). The experimental results demonstrated that Cyt *c*/CoOx NPs/GC biosensor exhibited electrocatalytic activity toward the reduction of hydrogen peroxide and application to hydrogen peroxide determination was exemplified.

Keywords Nanoparticle · Biosensor · Bioelectrochemistry · Electrochemical nanotechnology

A. Mohammadi · S. Ahadi
Department of Drug and Food Control, Faculty of Pharmacy, Tehran University of Medical Sciences, Tehran, Iran

A. Mohammadi · S. Ahadi
Pharmaceutical Quality Assurance Research Center, Faculty of Pharmacy, Tehran University of Medical Sciences, Tehran, Iran

A. B. Moghaddam (✉)
Department of Engineering Science, College of Engineering, University of Tehran, Tehran, Iran
e-mail: bayandori@gmail.com; bayandori@khayam.ut.ac.ir

A. Mohammadi · R. Dinarvand
Nanotechnology Research Centre, Faculty of Pharmacy, Tehran University of Medical Sciences, P.O. Box 14155/6451, Tehran, Iran

A. A. Khodadadi
Catalysis and Nanostructured Materials Research Laboratory, School of Chemical Engineering, University of Tehran, P.O. Box 11155/4563, Tehran, Iran

1 Introduction

Oxide semiconductor nanoparticles have received considerable attention in many fields [1–3]. They are suitable substrates for biomolecule immobilization due to their good biocompatibility and easy preparation. Nanostructured biointerfaces based on TiO_2 nanoneedles [4], TiO_2 [5], WO_3 [6], ZnO [7], and Fe_3O_4 [8] nanoparticles have been reported for sensing applications. Metal oxide nanomaterials have been extensively studied and used in many fields. They are emerging as promising candidates for various applications.

Electrochemical procedures are extensively applied to electrodepositing of oxide materials. Cobalt oxide-based films, in particular, have attracted a great interest in view of their potential applications [9]. Thus, cathodic electrodeposition of cobalt from aqueous solutions is a well-known process [10–12]. Alternatively, anodic electrodeposition of insoluble cobalt oxide/hydroxide has been investigated [13]. Electrodeposition of cobalt hydroxides on an inert conducting substrate, a neutral medium, seems to provide the best conditions for success. Electrodeposition of cobalt oxide/hydroxide film in 0.1 M acetate buffer solution containing of $CoCl_2$ at pH 7.3 has been reported [14]. Cobalt oxide-based materials are employed for making of electrochromic thin film [11], heterogeneous catalyst [15],

and magnetoresistive devices [16]. Choosing an electrochemical method for deposition of cobalt oxide film presents several advantages in comparison to other procedures [17].

The small redox proteins like azurin, ferredoxin, and cytochromes are natural electron shuttles for redox enzymes. Cytochrome *c* is a water-soluble heme protein that exists in cytosol between the inner and outer membranes of mitochondria. Additionally, it plays an important role in biological respiratory chain. In fact, its function is to receive electrons from the cytochrome *c* reductase and deliver them to cytochrome *c* oxidase [18].

Protein electrochemistry has become a powerful tool, both to study redox enzymes and make sensitive biosensor devices [19]. Because the proteins are huge molecules, electron transfer (ET) from redox center of a protein to the surface of an electrode is a problem. For optimal control of the oxidation state of cofactors and efficient relay of electrons to active site, fast interfacial ET is a prerequisite [20]. The modification of electrode surface by nanostructure materials as a mediator makes advantageous for the facility of direct ET between active centers of biomolecule and electrode surface [21]. Many efforts have been made to improve the ET characteristics of proteins [22–29].

Herein, we describe an electrochemical investigation of immobilized cytochrome *c* redox reaction on electrodeposited CoOx NPs. This is the first research concerning cytochrome *c* immobilization on CoOx NPs surface.

2 Experimental

2.1 Chemicals and reagents

Cytochrome *c* from horse heart was purchased from Sigma and used without further purification. KH_2PO_4, K_2HPO_4, CH_3COONa, CH_3COOH, $CoCl_2$, and the other reagents were received from Merck. Pure nitrogen gas was passed through the solution to avoid probable oxidation during the experiments. All solutions are prepared with distilled water.

2.2 Apparatus and procedure

Electrochemical experiments were performed using an electrochemical analyzer (μAUTOLAB TYPE III) connected to a personal computer with GPES software. Measurements were carried out at ambient temperature (25 ± 2 °C) in a conventional electrochemical cell consisting of a glassy carbon (GC) working electrode (disk, 1 mm in diameter), a platinum wire as counter electrode and Ag/AgCl/KCl as reference electrode (KCl-saturated, 0.197 V vs. a normal hydrogen electrode, NHE). All potentials are reported with respect to this reference electrode. Potassium phosphate buffer (KH_2PO_4 and K_2HPO_4; 50 mM total phosphate) at pH 7.0 was used as a background electrolyte.

AFM measurements were performed using a DME atomic force microscope with a Dual Scope C-21 controller and DS 95-50 scanner. Furthermore, SEM images were recorded using a ZEISS DSM 960 instrument.

2.3 Preparation of CoOx NPs/GC electrode

At first, GC surface was mechanically polished with 0.3 and 0.05 μm α-alumina powders on a polishing cloth and washed with distilled water. The electrode was then ultrasonicated in ethanol. Continuous voltammograms were recorded in 0.5 M H_2SO_4 between −0.5 and 1.1 V versus reference electrode at 200 mV s^{-1} until the repetitive voltammograms were obtained. The electrochemical deposition of cobalt oxide nanoparticles were performed from the phosphate buffer solution (PBS pH 7.0) containing of 1 mM $CoCl_2$ by consecutive CV (30 cycles) over a potential region of 0.5 to −1.0 V at 100 mV s^{-1} [9, 13, 17, 30]. As is well known, the surface-to-volume ratio of particles increases with the size reduction and due to the similar dimensions of biomolecules and nanostructures, the smaller nanoparticles play an important role during the immobilization process. Consequently, more voltammograms applied through the deposition process cause the growth of CoOx NPs into larger sizes (CoOx microparticles), which are not suitable for modification.

3 Results and discussions

3.1 Scanning electron microscopy (SEM) and atomic force microscopy (AFM)

In order to examine the formation of nanoparticles, surface analysis of electrodeposited CoOx NPs on the GC was examined by SEM and AFM techniques. Figure 1a shows the SEM image of GC surface previous to construction of CoOx NPs, while Fig. 1b of this figure shows the SEM image of CoOx NPs, electrodeposited on the electrode surface. An inset of Fig. 1b on the lower left corner demonstrates the SEM image of CoOx NPs in higher magnification. As can be seen, the nanoscale particles are grown by electrodeposition on the GC surface. The same modified electrode has been used to obtain AFM images. In order to three-dimensional (3D) image of the surface topography in Fig. 2, as well as small nanoparticles distributed on the surface, larger agglomerated particles are also observed on it.

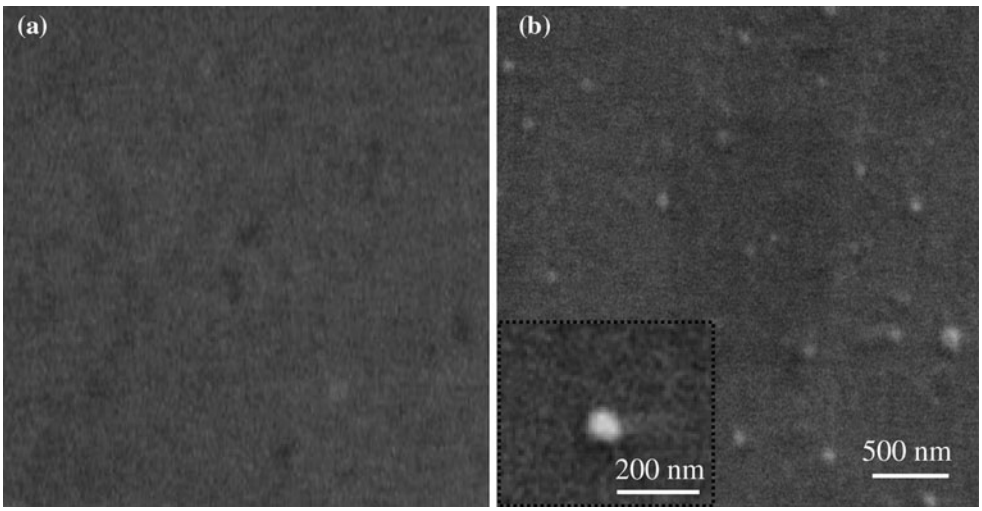

Fig. 1 SEM image of glassy carbon surface **a** before construction of CoOx NPs, **b** after electrodeposition of CoOx NPs. *Inset* is the SEM image with higher magnification

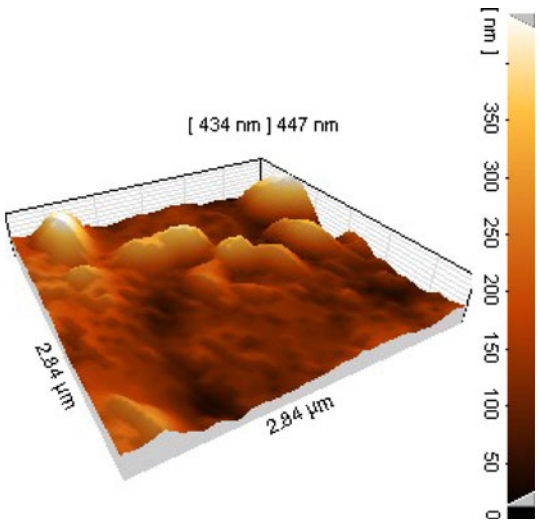

Fig. 2 Three-dimensional (3D) AFM image of the electrodeposited CoOx NPs on glassy carbon surface

Figure 3b shows a profile for selected direction corresponding to arrow from the AFM image of Fig. 3a. It shows CoOx NPs diameter for selected points of profile with 255 nm. Figure 3c shows an image height distribution from Fig. 3a. These images indicate that the CoOx NPs size varies from under 50 nm to slightly less than 300 nm.

3.2 Redox behavior of cytochrome *c* after immobilization on the surface of CoOx NPs/GC electrode

The CoOx NPs/GC electrode was immersed in fresh phosphate solution containing 5 mg mL^{-1} cytochrome *c*, and the immobilization of protein molecules was performed by consecutive CV (30 cycles) over a suitable potential region of 0.70 to −0.60 V at 100 mV s^{-1}. Afterward, the Cyt *c*/CoOx NPs/GC electrode was washed with distilled water to perform other studies. The ability of immobilized cytochrome *c* to exchange electrons with CoOx NP surfaces at various scan rates was investigated using voltammetry. Figure 4 shows the comparative CVs of three electrodes in PBS at 40 mV s^{-1}. Figure 4a shows the CVs of pure GC electrode, while Fig. 4b related to the voltammogram of CoOx NPs/GC electrode before the immobilization of protein on their surface. The augmentation of base line current in this voltammogram in comparison with Fig. 4a is attributed to the increase of the active surface area of electrode due to the presence of CoOx NPs on its surface. Neither the bare GC electrode nor CoOx NPs/GC electrode shows any electrochemical response. In accordance to Fig. 4c, Cyt *c*/CoOx NPs/GC electrode has one pair of redox waves corresponds to conversion between Cyt *c*-Fe(III) and Cyt *c*-Fe(II). In agreement with data in Fig. 4, it is revealed that CoOx NPs have an important role in direct ET reactivity of immobilized protein molecules.

At the scan rate of 100 mV s^{-1}, reductive and oxidative peaks are located at −264 and 85 mV, respectively, with ΔE, an indication of ET rate, of 349 mV. The large peak separation may be related to the immobilization of protein molecules in an abnormal orientation [31]. Its formal potential, $E^{\circ'}$ (defined as the average of reductive and oxidative peaks), is calculated to be −89.5 mV with respect to the reference electrode (107.5 mV vs. NHE). The formal potential is more positive than that of cytochrome *c* on gold nanoparticles–chitosan–carbon nanotubes (37 mV vs. NHE) [32]. Possibly, the presence of special interaction between cytochrome *c* and CoOx NPs can affect the microenvironment of prosthetic group and

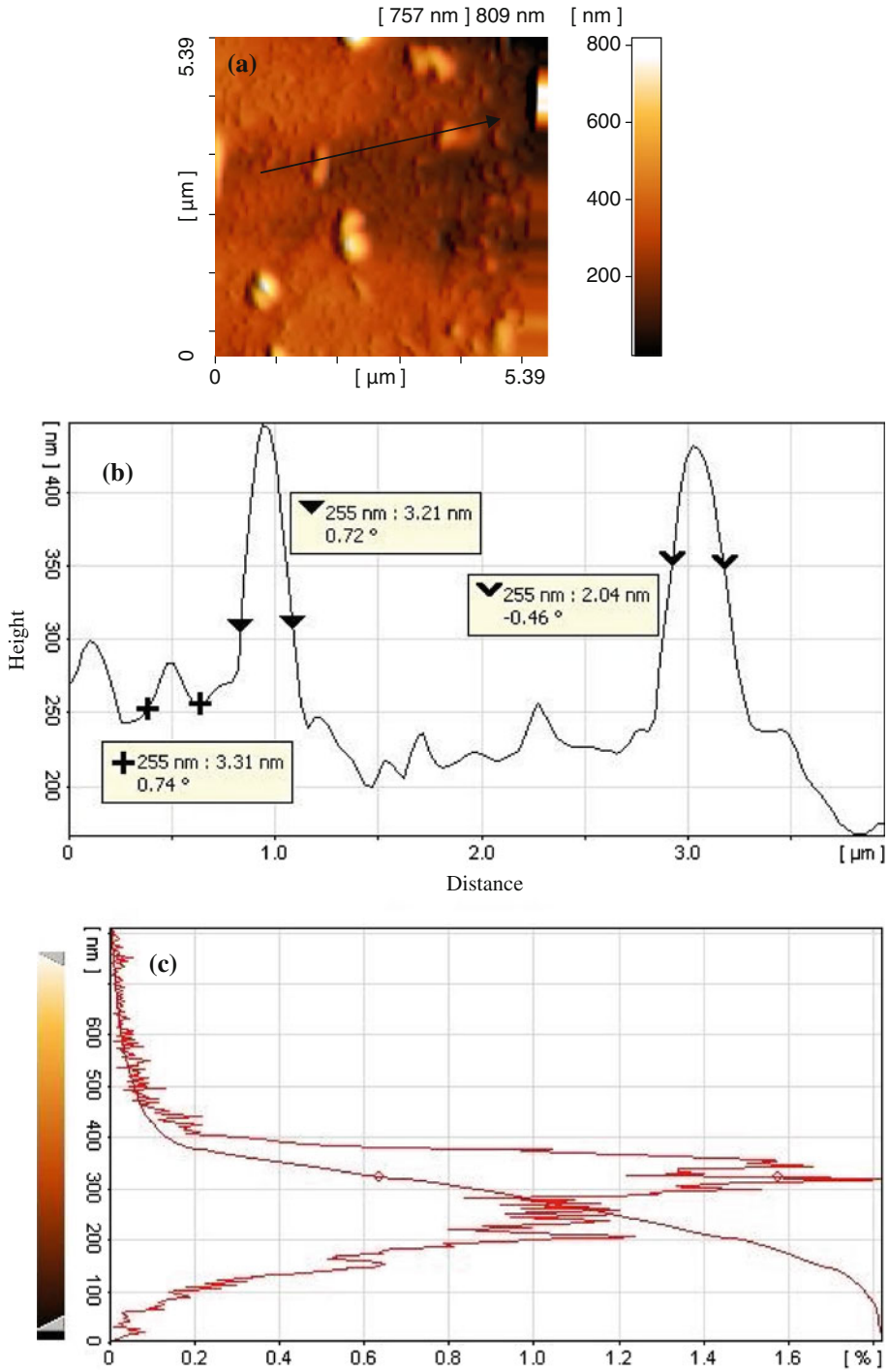

Fig. 3 **a** AFM image of electrodeposited CoOx NPs on glassy carbon surface, **b** obtained image profile for selected direction by *arrow* from **a**, **c** Image height distribution from **a**

make $E^{\circ'}$ of cytochrome *c* shifting [33, 34]. Formal potentials for horse cytochrome *c* and yeast cytochrome *c* on the indium/tin oxide (ITO) were −28 mV (169 mV vs. NHE) and −48 mV (149 mV vs. NHE), respectively [35]. This value for yeast iso-1 cytochrome *c* on bare gold with 4,4′-dipyridyl as a facilitator was 290 mV versus NHE [20], it was 108 mV (305 mV vs. NHE) for cytochrome *c* on TiO_2 nanoneedles [4], and it was 194 mV (391 mV vs. NHE) for cytochrome *c* on L-cysteine modified electrode [36]. Figure 5a shows the recorded cyclic voltammograms of Cyt *c*/CoOx NPs/GC electrode at different scan rates from 10 to 90 mV s^{-1}. With scan rate augmentation, the redox peak currents of immobilized cytochrome *c* increased, accompanied a little enlarged peak-to-peak separation (ΔE). Scan rate dependence of peaks is plotted in Fig. 5b. At scan rates from 40 to 1100 mV s^{-1}, redox peak currents showed linear response to scan rate, which is characteristic of a thin layer electrochemical behavior

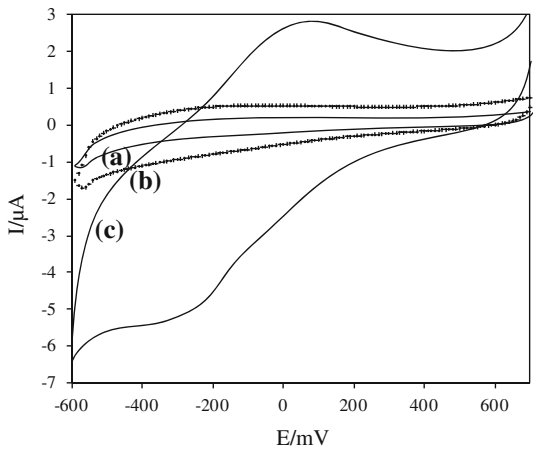

Fig. 4 Comparative CVs at 40 mV s^{-1} in PBS for three electrodes; (*a*) GC, (*b*) CoOx NPs/GC, and (*c*) Cyt *c*/CoOx NPs/GC electrodes

[37]. The linear regression equations were $i_{pc} = -0.0356\ v - 0.989$ (correlation coefficient was 0.995) and $i_{pa} = 0.0366\ v + 1.107$ (correlation coefficient was 0.996). Thus, electrochemical reaction corresponds to a surface-controlled process and immobilized cytochrome *c* was stable. To obtain the kinetic parameters of immobilized cytochrome *c*, scan rates were increased. Through scan rate increase, peak separation between oxidative and reductive peak potentials was increased. At higher scan rates ($v > 1.2$ V s^{-1}), peak potentials versus the logarithm of scan rates are linear. It is in agreement with Laviron theory, with slopes of $-2.3RT/\alpha nF$ and $2.3RT/(1-\alpha)nF$ for reductive and oxidative peaks, respectively [38]. *R*, *T*, and *F* possess their conventional meanings. Subsequently, αn is calculated to be 0.42. Given $0.3 < \alpha < 0.7$, in general [39], it could be concluded that $n = 1$ and $\alpha = 0.42$.

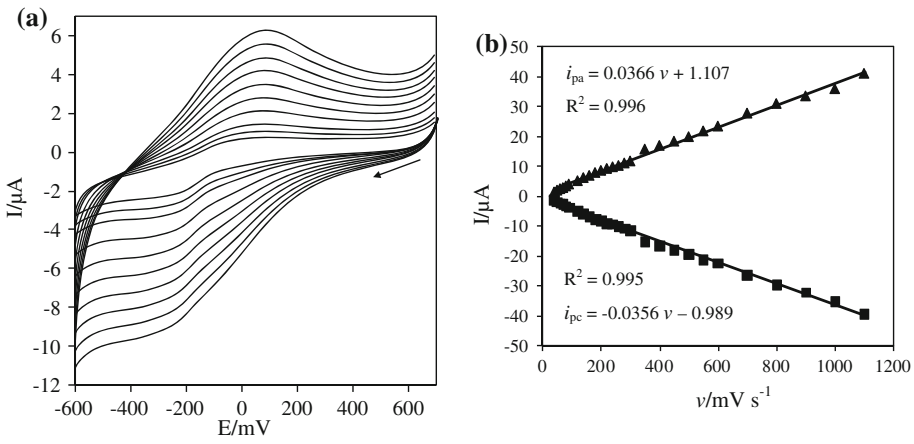

Fig. 5 **a** CVs of Cyt *c*/CoOx NPs/GC electrode in PBS at different scan rates, from inner to outer; 10, 15, 20, 30, 40, 50, 60, 70, 80, and 90 mV s^{-1}, **b** relationship between peak currents (i_{pa}, i_{pc}) versus scan rates

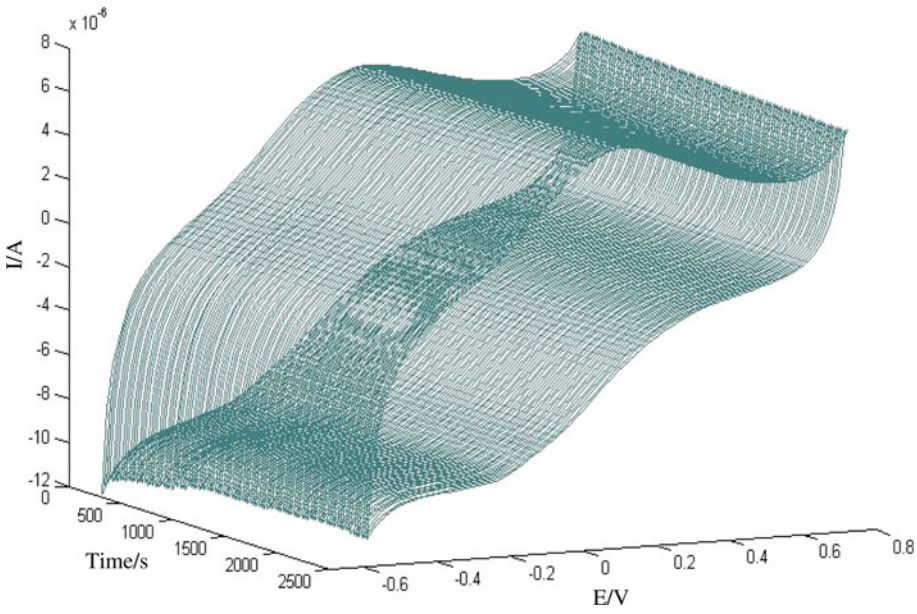

Fig. 6 Continuous CVs at 100 mV s^{-1} of Cyt *c*/CoOx NPs/GC electrode in PBS

Therefore, the charge-transfer coefficient (a) was estimated as 0.42. Figure 6 shows the continuous CVs of Cyt c/CoOx NPs/GC. The oxidative and reductive peak currents remain more or less stable with cycling and there are no changes in redox potentials. This voltammograms indicate the stability of immobilized protein on Cyt c/CoOx NPs/GC.

In accordance to Fig. 7, the surface area, under 50th voltammogram, was almost 3.2% smaller than first voltammogram. This differentiation reduced to 0.7% for same comparison about 50th and 100th voltammograms. There were no differences between 100th and 150th voltammograms at 100 mV s^{-1}, because the surface area of voltammogram indicates the consumed charge (Q), related to amount of immobilized protein. Therefore, this figure confirms that the immobilized protein molecules have good stability.

3.3 Application of Cyt c/CoOx NPs/GC electrode for electrocatalytic reduction of H_2O_2

It has been reported that proteins containing heme prosthetic groups, like HRP, myoglobin, cytochrome c, hemoglobin, and catalase could be used as biocatalyzers to catalyze the reduction of H_2O_2 [40, 41]. In this research, electrochemical catalytic reduction of H_2O_2 with cytochrome c was assessed by cyclic voltammetry (CV) at scan rate of 100 mV s^{-1}. Figure 8 exhibits a redox couple of Cyt c ($Fe^{III/II}$) in the absence of analyte. Upon the addition of analyte, a growth in the reduction peak of H_2O_2 appeared. It shows that electrocatalytic reduction of H_2O_2 took place at Cyt c (Fe^{II}).

Further experimental results showed that the catalytic currents increased linearly with H_2O_2 concentration increase in solution (Fig. 8, inset). It is importance to

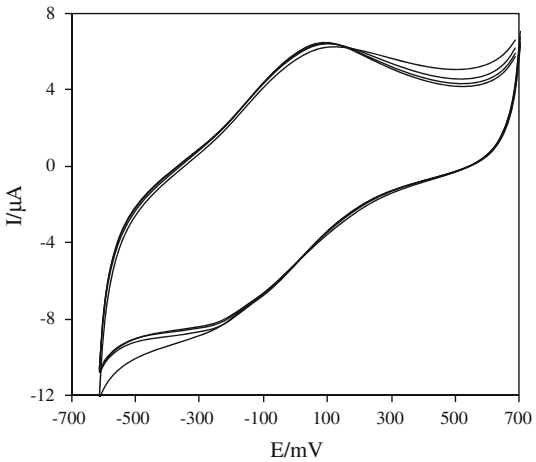

Fig. 7 Continuous CVs at 100 mV s^{-1} of Cyt c/CoOx NPs/GC electrode, from outer to inner the 1st, 50th, 100th, and 150th CV in PBS

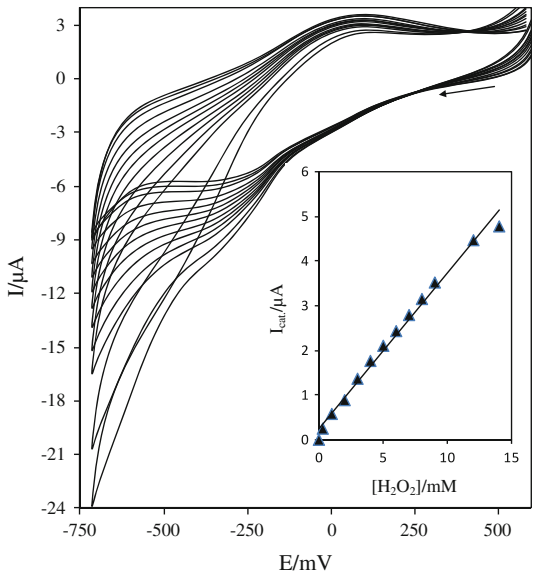

Fig. 8 CVs corresponding to electrochemical responses of Cyt c/CoOx NPs/GC generated by different H_2O_2 concentrations in PBS from inner to outer; 0.0, 0.3, 1.0, 2.0, 3.0, 4.0, 5.0, 6.0, 7.0, 8.0, 9.0, 12.0, and 14.0 mM, at 100 mV s^{-1}. *Inset*; catalytic current at −400 mV versus H_2O_2 concentration

mention that the oxidative peak did not disappear after onset reductive catalysis. It could be attributed that the some of adsorbed protein is probably not catalytically active. The catalytic peak currents were proportional to the concentration of H_2O_2 with a linear range from 0.3 to 12.0 mM. It can be seen from the inset of Fig. 8 that the response of biosensor is nonlinear for the concentrations greater than 12 mM of hydrogen peroxide. The linear ranges for catalytic reduction of H_2O_2 are 0.1–5.0 mM (cyclic voltammetric analysis) and 0.85–24000 μM (amperometric analysis) for catalase/NiO nanoparticles [42] and cytochrome c/TiO_2 nanoneedles [4], respectively. Also, linear range values of 0.2–7 mM [43], 0.01–3 mM [44], 0.01–1.1 mM [45], 0.005–2 mM [46], 0.05–0.4 mM [47], and 0.1–5 mM [48] for H_2O_2 determination with various modified electrodes have been reported.

The linear regression equation was $I_p = 0.370\,[H_2O_2] + 0.179$ with a correlation coefficient of 0.996 (12 points). Calibration plot is linear for a wide range of H_2O_2 concentration. Relative standard deviation (%RSD) is 2.3% for six successive determinations at 10 mM H_2O_2. Sensitivity and detection limit (3σ) of the biosensor toward H_2O_2 were found to be 0.370 μA mM^{-1} and 80 μM, respectively.

4 Conclusions

Cobalt oxide nanoparticles (CoOx NPs) were electrodeposited on the surface of GC electrode and assessed using SEM and AFM procedures. The CoOx NPs showed strong

adsorption to cytochrome *c*, leading to great enhancement of enzyme loading and improvement of its behavior due to their excellent biocompatibility. Therefore, they have potential applications in bioelectrochemistry, biosensors, and bioelectronics. The resulting biosensor exhibited good performance for electrocatalytic reduction of H_2O_2. The direct electrochemistry of cytochrome *c* in the form of Cyt *c*/CoOx NPs/GC was assessed by CV. The proportionality of peak currents to scan rate and constancy of integration of reduction peaks at different scan rates represent the characteristics of diffusion less and thin layer electrochemical behavior. Cyt *c*/CoOx NPs/GC showed a satisfactory sensitivity and reproducibility for H_2O_2.

Acknowledgments The financial support was provided by the Tehran University of Medical Sciences. Research Affairs are gratefully acknowledged.

References

1. Latonen RM, Esteban BM, Kvarnstrom C, Ivaska A (2009) J Appl Electrochem 39:653
2. Nabid MR, Golbabaee M, Bayandori Moghaddam A, Mahdavian AR, Amini MM (2009) Polym Comp 30:841
3. Bayandori Moghaddam A, Ganjali MR, Saboury AA, Moosavi-Movahedi AA, Norouzi P (2008) J Appl Electrochem 38:1233
4. Luo Y, Liu H, Rui Q, Tian Y (2009) Anal Chem 81:3035
5. Shi YT, Yuan R, Chai YQ, Tang MY, He XL (2007) J Electroanal Chem 604:9
6. Deng Z, Gong Y, Luo Y, Tian Y (2009) Biosens Bioelectron 24:2465
7. Dai ZH, Shao GJ, Hong JM, Bao JC, Shen J (2009) Biosens Bioelectron 24:1286
8. Cao D, Hu N (2006) Biophys Chem 121:209
9. Casella IG, Gatta M (2002) J Electroanal Chem 534:31
10. Yoshino T, Baba N (1995) Sol Energy Mater Sol Cells 39:391
11. Monk PMS, Ayub S (1997) Solid State Ion 99:115
12. Gomez E, Marin M, Sanz F, Valles E (1997) J Electroanal Chem 422:139
13. Barbero C, Planes GA, Miras MC (2001) Electrochem Commun 3:113
14. Casella IG, Guascito MR (1999) J Electroanal Chem 476:54
15. Casella IG, Guascito MR (1999) Electrochim Acta 45:1113
16. Ueda Y, Kikuchi N, Ikeda S, Houga T (1999) J Magn Mater 198:740
17. Casella IG (2002) J Electroanal Chem 520:119
18. Santucci R, Brunori M (1992) Bioelectrochem Bioenerg 29:177
19. Heering HA, Hirst J, Armstrong FA (1998) J Phys Chem B 102:6889
20. Heering HA, Wiertz FGM, Dekker C, de Vries S (2004) J Am Chem Soc 126:11103
21. Li JH, Gui Y, Wang MJ, Sun CY (2006) In: Grimes CA, Dickey EC, Pishko MV (eds) Electrochemical sensor. American Scientific Publishers, California
22. Armstrong FA, Hill HAO, Walton NJ (1988) Acc Chem Res 21:407
23. Rusling JF (1998) Acc Chem Res 31:363
24. Cai J, Du D (2008) J Appl Electrochem 38:1217
25. Mohammadi A, Bayandori Moghaddam A, Dinarvand R, Rezaei-Zarchi S (2009) Int J Electrochem Sci 4:895
26. Mohammadi A, Bayandori Moghaddam A, Kazemzad M, Dinarvand R, Badraghi J (2009) Mat Sci Eng C 29:1752
27. Du D, Cai J, Song D, Zhang A (2007) J Appl Electrochem 37:893
28. Hirst J, Armstrong FA (1998) Anal Chem 70:5062
29. Mohammadi A, Bayandori Moghaddam A, Dinarvand R, Badraghi J, Atyabi F, Saboury AA (2008) Int J Electrochem Sci 3:1248
30. Salimi A, Hallaj R, Soltanian S (2007) Biophys Chem 130:122
31. Sun W, Wang D, Li G, Zhai Z, Zhao R, Jiao K (2008) Electrochim Acta 53:8217
32. Xiang C, Zou Y, Sun LX, Xu F (2007) Talanta 74:206
33. Zhang Z, Rusling JF (1997) Biophys Chem 63:133
34. Nassar AEF, Zhang Z, Hu N, Rusling JF, Kumosinski TF (1997) J Phys Chem B 101:2224
35. Kasmi AE, Leopold MC, Galligan R, Robertson RT, Saavedra SS, Kacemi KE, Bowden EF (2002) Electrochem Commun 4:177
36. Liu YC, Cui SQ, Zhao J, Yang ZS (2006) Bioelectrochemistry 71:121
37. Bard AJ (1984) Electroanalytical chemistry. Marcel Dekker, New York
38. Laviron E (1979) J Electroanal Chem 101:19
39. Ma HY, Hu NF, Rusling JF (2000) Longmuir 16:4969
40. Prakash PA, Yogeswaran U, Chen SM (2009) Talanta 78:1414
41. Shie JW, Yogeswaran U, Chen SM (2009) Talanta 78:896
42. Salimi A, Sharifi E, Noorbakhsh A, Soltanian S (2007) Biophys Chem 125:540
43. Bayandori Moghaddam A, Ganjali MR, Dinarvand R, Ahadi S, Saboury AA (2008) Biophys Chem 134:25
44. Xiao P, Garcia BB, Guo Q, Liu D, Cao G (2007) Electrochem Commun 9:2441
45. Xiang C, Zou Y, Sun LX, Xu F (2009) Sens Actuat B 136:158
46. Yang YH, Yang MH, Jiang JH, Shen GL, Yu RQ (2005) Chin Chem Lett 16:951
47. Rezaei-zarchi S, Saboury AA, Javed A, Barzegar A, Ahmadian S, Bayandori Moghaddam A (2008) J Biosci 33:279
48. Safavi A, Maleki N, Moradlou O, Sorouri M (2008) Electrochem Commun 10:420